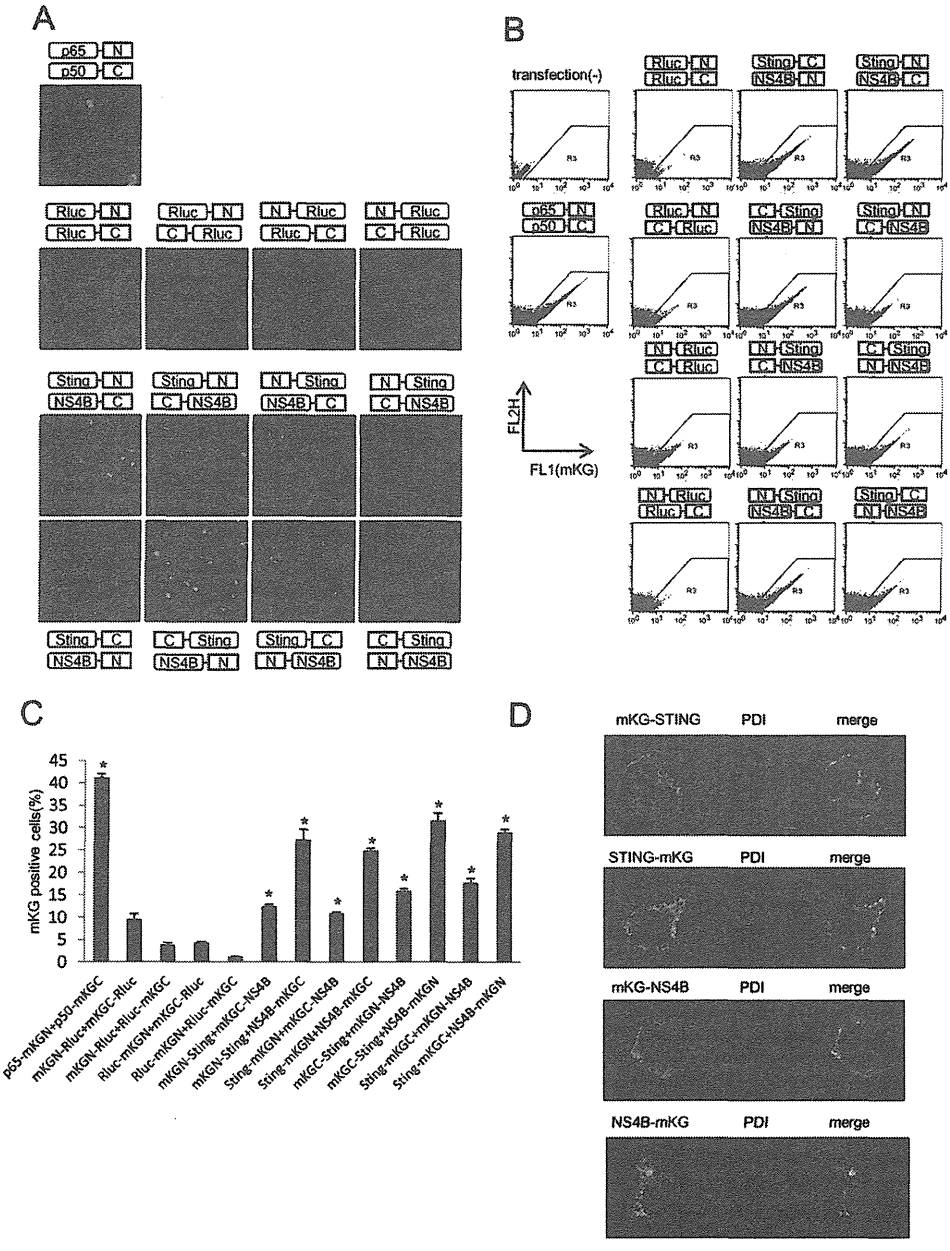

Fig. 3. BiFC assays of STING and NS4B. The complementary pairs of N- or C-terminally mKG-fused NS4B and STING expression plasmids were cotransfected in HEK293T cells. After 24 hours, the cells were fixed and observed by confocal microscopy (A) or subjected to flow cytometry to measure mKG-emitted fluorescence (BiFC signal) and to count BiFC signal-positive cells (B,C). Plasmids expressing p65-mKGN and p50-mKGC individually were used as a BiFC-positive control and plasmids expressing N- or C-terminally mKG fused Rluc were used as a negative control. The letters N and C denote complimentary N- and C-terminal fragments of mKG, respectively. Assays were performed in triplicate and error bars indicate the mean ± SD. Scale bars indicate 10 μm (A). *$P < 0.05$ compared with corresponding negative controls. (D) Plasmids expressing mKG fragment-fused STING or NS4B were transfected in HEK293T cells. After 24 hours, the cells were fixed and immunostained with anti-mKG and anti-PDI (ER) antibody. Nuclei were stained with DAPI. Cells were observed by confocal microscopy. Scale bars = 5 μm.

between NS4B, Cardif, and STING. To detect those interactions in living cells, we performed BiFC assays.[37,38] We constructed NS4B, Cardif, and STING expression plasmids that were N- or C-terminally fused with truncated mKG proteins, respectively. First, we cotransfected several different pairs of NS4B and STING expression plasmids that were fused with complementary pairs of N- or C-terminally truncated mKG. Strong fluorescence by mKG complexes (BiFC signal) was detected in all pairs of cotransfections, suggesting significant molecular interaction (Fig. 3A). In flow cytometry, all pairs of NS4B- and STING-mKG fusion proteins were positive for strong BiFC signal (Fig. 3B). The percentages of cells positive for BiFC signal were significantly higher in STING-mKG and NS4B-mKG fusion complexes than in corresponding controls (Fig. 3C). These results demonstrate that HCV-NS4B and STING proteins interact with each other strongly and specifically in cells. Fluorescence microscopy indicated that N- and C-terminal fusion of mKG onto NS4B and STING did not affect subcellular localization (Fig. 3D).

We next studied the molecular interaction between NS4B and Cardif by BiFC assay using NS4B and Cardif fusion plasmids that were tagged with complementary pairs of truncated mKG. Weak fluorescence was detected in cells transfected with the pairs N-Cardif and NS4B-C, N-Cardif and C-NS4B, C-Cardif and

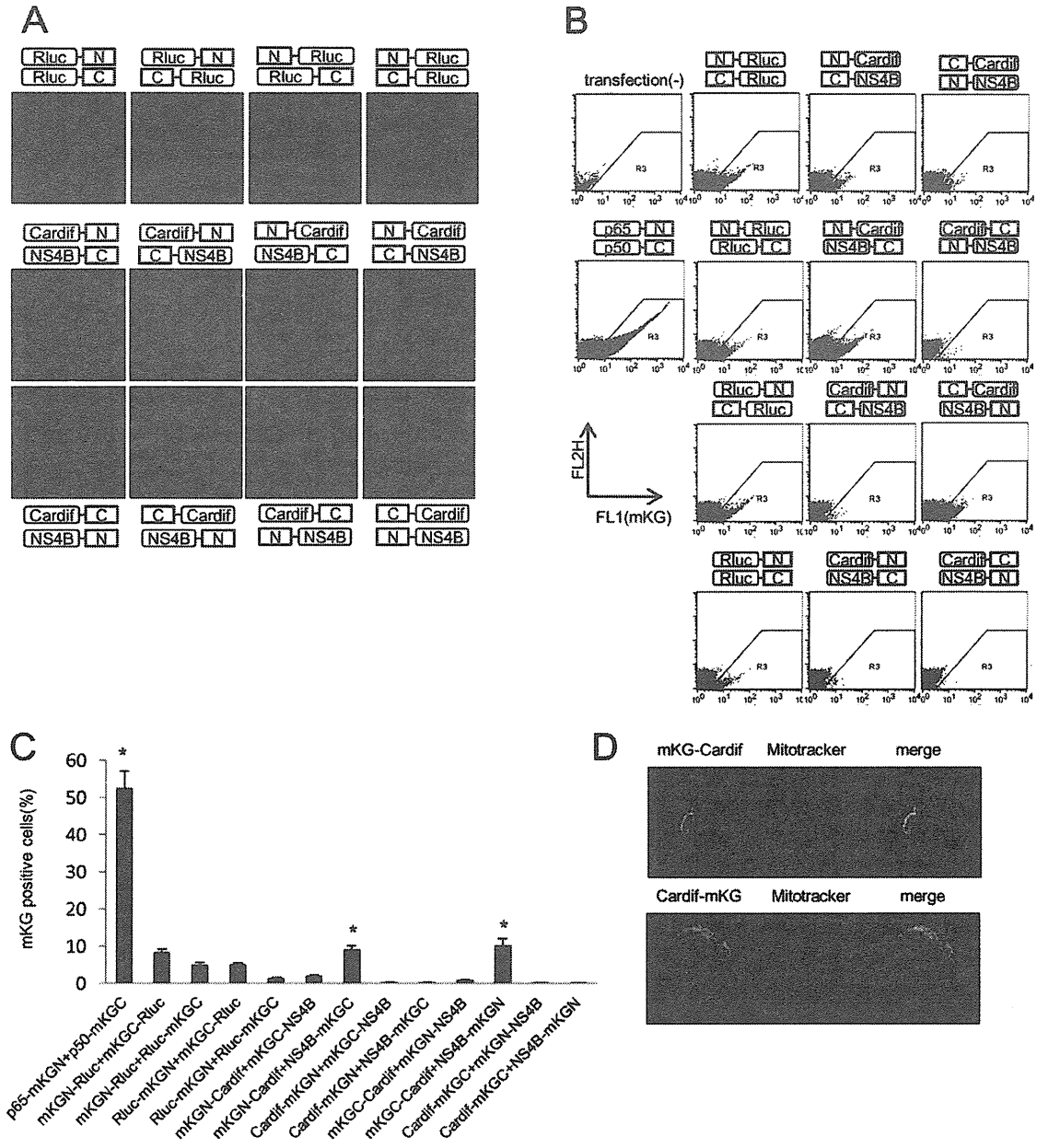

Fig. 4. BiFC assays of Cardif and NS4B. The complementary pairs of N- or C-terminally mKG-fused NS4B and Cardif expression plasmids were cotransfected in HEK293T cells. After 24 hours, the cells were fixed and observed by confocal microscopy (A) or subjected to flow cytometry to measure mKG-emitted fluorescence (BiFC signal) and to count BiFC signal-positive cells (B,C). Plasmids expressing p65-mKGN and p50-mKGC individually were used as a BiFC-positive control and plasmids expressing N- or C-terminally mKG-fused Rluc were used as a negative control. The letters N and C denote complimentary N- and C-terminal fragments of mKG, respectively. Assays were performed in triplicate, and error bars indicate the mean ± SD. Scale bars indicate 10 μm (A). *$P < 0.05$ compared with corresponding negative controls. (D) Plasmids expressing mKG fragment-fused STING or NS4B were transfected in HEK293T cells. After 24 hours, the cells were fixed and immunostained with anti-mKG antibody. Mitochondria were stained using Mitotracker, and nuclei were stained with DAPI. Cells were observed by confocal microscopy. Scale bars = 5 μm.

NS4B-N, and C-Cardif and N-NS4B (Fig. 4A,B). The percentage of cells positive for BiFC signal increased with the combination of N-Cardif and NS4B-C, and C-Cardif and NS4B-N (Fig. 4C). Fluorescence microscopy indicated that mKG-Cardif, but not Cardif-mKG, was partially colocalized with mitochondria, possibly due to disruption of mitochondria anchor domain by C-terminal fusion with mKG (Fig. 4D). These results indicate the lack of significant molecular interactions between NS4B and Cardif.

Binding of NS4B to STING Blocks Molecular Interaction Between Cardif and STING. It has been reported that STING binds Cardif directly.[20,22] Thus, we hypothesized that NS4B, through a competitive

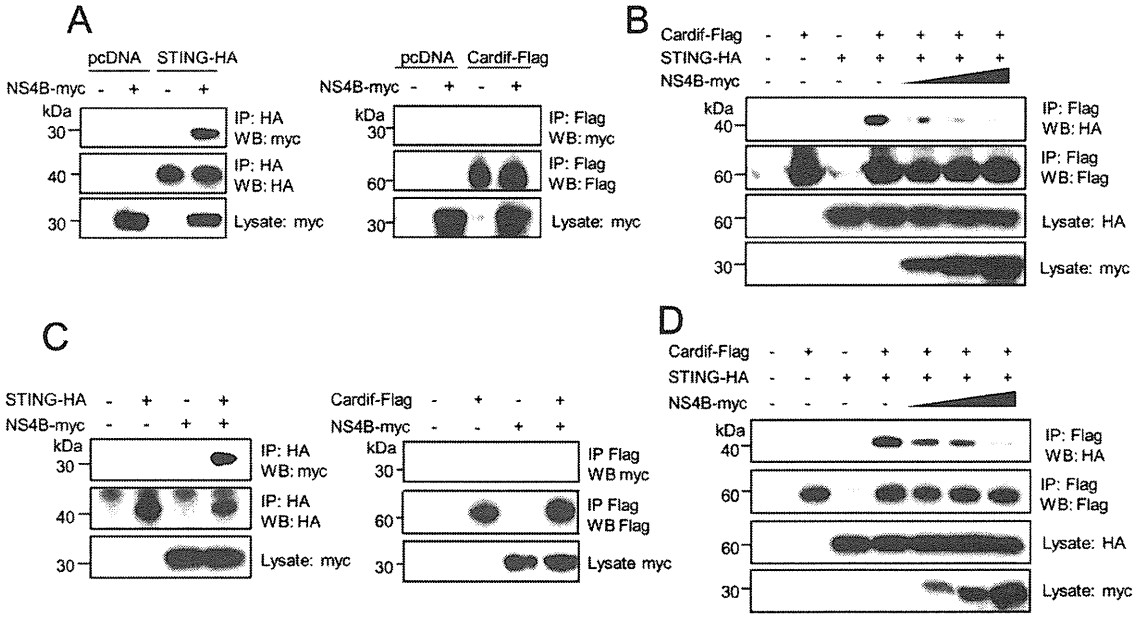

Fig. 5. Binding of NS4B to STING blocks molecular the interaction between Cardif and STING. (A,C) NS4B expression plasmid was cotransfected with STING or Cardif expression plasmid into HEK293T cells (A) or Huh7 cells (C). After 24 hours, cell lysates were subjected to immunoprecipitation using anti-HA or anti-Flag and were immunoblotted with anti-myc. (B,D) Cardif and STING expression plasmids were cotransfected with various amounts of NS4B plasmid in HEK293T cells (B) or Huh7 cells (D). After 24 hours, cells lysates were subjected to immunoprecipitation using anti-Flag and were immunoblotted with anti-HA.

interaction with STING, may hinder the direct molecular interaction between Cardif and STING. To verify this hypothesis, we performed immunoprecipitation assays. First, we transfected plasmids that expressed NS4B and Cardif, or NS4B and STING, in HEK293T cells or Huh7 cells, and performed immunoprecipitation. NS4B strongly bound to STING in both HEK293T cells and Huh7 cells, suggesting specific molecular interactions, whereas NS4B and Cardif did not show any obvious interaction (Fig. 5A,C). Consistent with previous reports, STING and Cardif showed significant interaction (Fig. 5B,D). Interestingly, those interactions were decreased by coexpression of NS4B, depending on its input amount, and finally blocked completely in both HEK293T and Huh7 cells (Fig. 5B,D). Collectively, the results above demonstrate that NS4B disrupts the interaction between Cardif and STING possibly through competitive binding to STING.

Effects on HCV Infection and Replication Levels by STING Knockdown and NS4B Overexpression. We next studied the impact of STING-mediated IFN production and its regulation by NS4B on HCV infection and cellular replication. First, we transfected three STING-targeted siRNAs into Huh7/Feo cells (Fig. 6A). As shown in Fig. 6B, STING knockdown cells conferred significantly higher permissibility to HCV replication. We next transfected HCV-JFH1 RNA into Huh7 cells that were transiently transfected with NS4B. As shown in Fig. 6C, HCV core protein expression was significantly higher in NS4B-overexpressed cells. Furthermore, HCV replication was increased significantly in Huh7/Feo cells overexpressing NS4B (Fig. 6D). Taken together, the results above demonstrate that STING and NS4B may negatively or positively regulate cellular permissiveness to HCV replication.

The N-terminal Domain of NS4B Is Essential for Suppressing IFN-β Promoter Activity Mediated by RIG-I, Cardif, and STING. It has been reported that the N-terminal domain of several forms of flaviviral NS4B shows structural homology with STING.[24] We therefore investigated whether the STING homology domain in NS4B is responsible for suppression of IFN-β production. We constructed two truncated NS4B expression plasmids, which covered the N terminus (NS4Bt1-84, amino acids 1 through 84) containing the STING homology domain and the C terminus (NS4Bt85-261, amino acids 85 through 261), respectively (Fig. 7A). Immunoblotting showed that NS4Bt1-84 and NS4Bt85-261 yielded protein bands of ~9 kDa and ~20 kDa, respectively. Aberrant bands in the truncated NS4B may be due to alternative post-translational processing. HEK293T cells were transfected with ΔRIG-I, Cardif, or STING, and NS3/4A or the truncated NS4B, along with IFN-β-Fluc plasmid, and a reporter assay was performed. NS4Bt1-84 significantly suppressed RIG-I, Cardif, and STING-

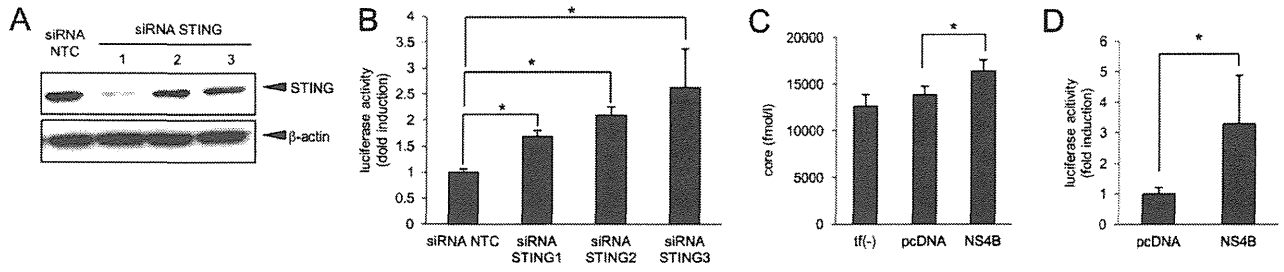

Fig. 6. Effects on HCV replication levels by STING knockdown and NS4B overexpression. (A) Effects of siRNA knockdown of STING by siRNA. Huh7 cells were transfected with STING-targeted siRNAs (siRNA STING-1, -2, and -3, respectively) or negative control siRNA (siRNA NTC). Seventy-two hours after transfection, cells were harvested and expression levels of STING protein were detected by immunoblotting. (B) Huh7 cells expressing HCV-Feo subgenomic replicon (Huh7/Feo)[27,28] were transfected with STING-targeted siRNAs or negative control siRNA. Seventy-two hours after transfection, cells were harvested, and internal luciferase activities were measured. The *y* axis indicates luciferase activity shown as a ratio of transfection-negative control. Assays were performed in triplicate, and error bars indicate the mean + SD. $*P < 0.05$ compared with corresponding negative controls. (C) Empty plasmid or plasmid expressing NS4B was transfected into Huh7 cells. After 24 hours, HCV-JFH1 RNA was transfected into these cells. Seventy-two hours after virus transfection, HCV core antigen levels in culture medium were measured. Assays were performed in triplicate, and error bars indicate the mean + SD. $*P < 0.05$ compared with corresponding negative controls. tf(−), transfection-negative control. (D) Huh7 cells expressing HCV-Feo replicon (Huh7/Feo)[27,28] were transfected with NS4B expressing plasmid or empty plasmid (pcDNA). Forty-eight hours after transfection, internal luciferase activities were measured. The *y* axis indicates luciferase activity shown as a ratio of the transfection-negative control. Assays were performed in triplicate, and error bars indicate the mean + SD. $*P < 0.05$ compared with corresponding negative controls.

induced IFN-β promoter activity, whereas NS4Bt85-261 did not (Fig. 7B). These results suggest that the N-terminal domain of NS4B is responsible for association with STING. Fluorescent microscopy indicated that both NS4Bt1-84 and NS4Bt85-26 colocalized with ER and STING (Fig. 7C).

NS4B Suppresses IFN Production Signaling Cooperatively with NS3/4A. It has been reported that

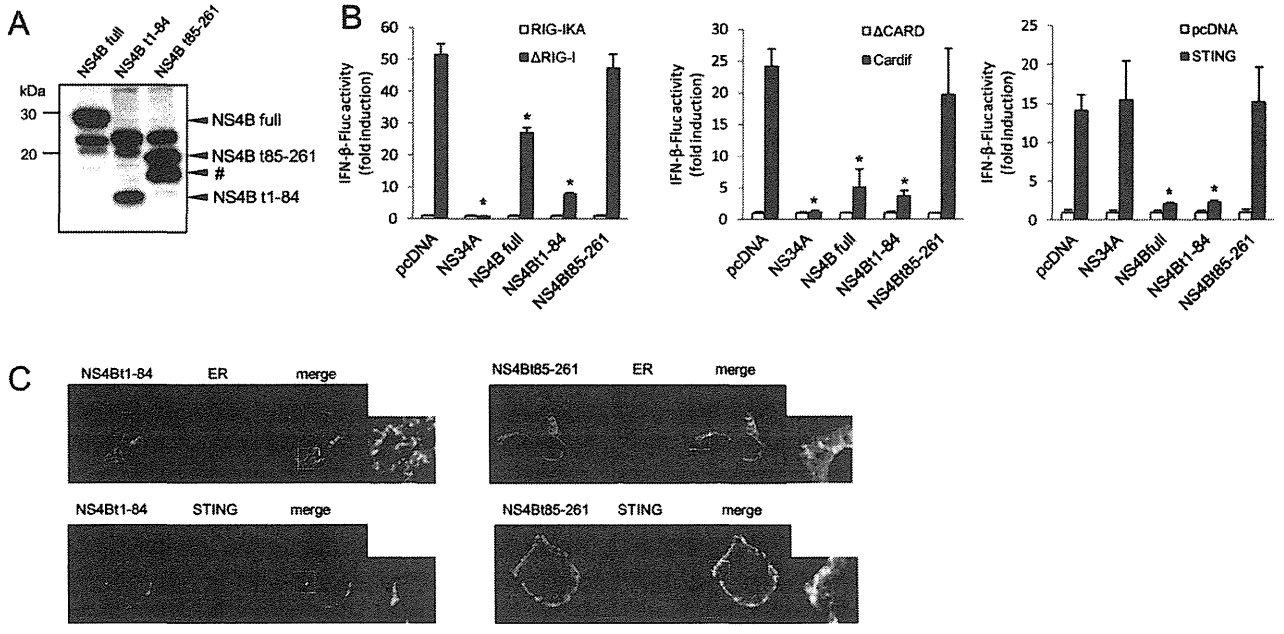

Fig. 7. The N-terminal domain of NS4B is essential for suppressing IFN-β promoter activity induced by RIG-I, Cardif, or STING. (A) Immunoblotting of NS4B and truncated NS4B, NS4B t1-84, and NS4Bt85-216. HEK293T cells were transfected with NS4B or truncated NS4B. After 24 hours, the cells were lysed and immunoblot assays were performed. The band indicated by the pound sign (#) is a truncated NS4B, probably generated via alternative posttranslational processing. (B) Plasmids expressing ΔRIG-I, Cardif, or STING as well as NS3/4A or the indicated truncated form of NS4B were cotransfected with pIFN-β-Fluc and pRL-CMV in HEK293T cells. Dual luciferase assays were performed 24 hours after transfection. Plasmids expressing RIG-IKA, ΔCARD, or pcDNA were used as negative controls. The *y* axis indicates IFN-β-Fluc activity shown as relative values. Assays were performed in triplicate, and error bars indicate the mean ± SD. $*P < 0.05$ compared with corresponding negative controls. (C) Plasmids expressing NS4Bt1-84-myc of NS4Bt85-261-myc were transfected with or without plasmids expressing HA-STING in HEK293T cells. After 24 hours, the cells were fixed and immunostained. Nuclei were stained with DAPI. Cells were observed by confocal microscopy. Scale bars indicate 5 μm.

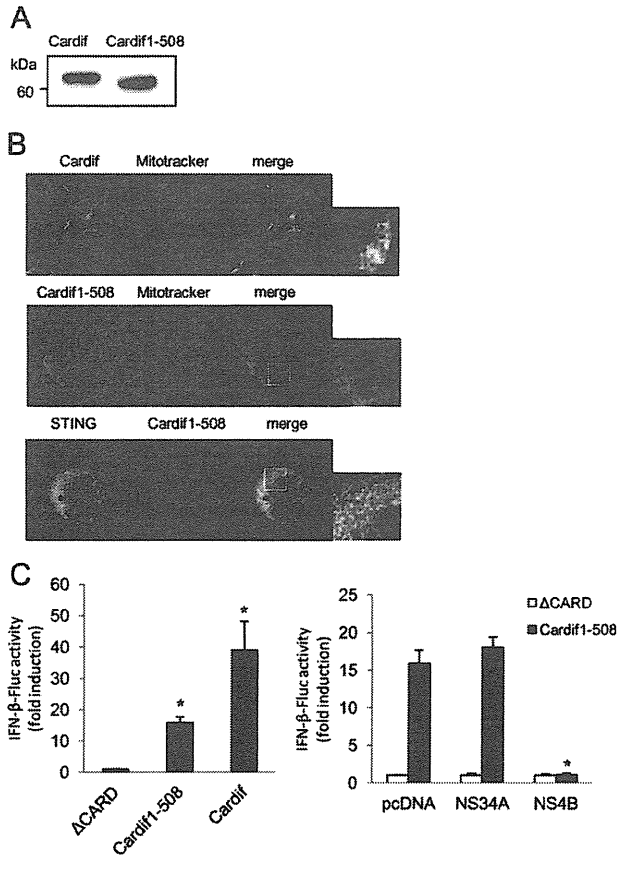

Fig. 8. NS4B suppressed IFN-β production pathway independently of and cooperatively with NS3/4A. (A) Immunoblotting of Cardif and truncated Cardif (Cardif1-508). HEK293T cells were transfected with Cardif or truncated Cardif (Cardif1-508). After 24 hours, the cells were lysed and immunoblot assays were performed. (B) Subcellular localization of Cardif and truncated Cardif (Cardif1-508). HEK293T cells were immunostained with anti-Cardif antibody or HEK293T cells were transfected with myc-tagged truncated Cardif (Cardif1-508-myc), and after 24 hours the cells were immunostained with anti-myc. Mitochondria were stained with Mitotracker (red) and nuclei were stained with DAPI (blue). Plasmid expressing myc-tagged truncated Cardif (Cardif1-508) and plasmid expressing HA-tagged STING were transfected into HEK293T cells. The cells were immunostained with anti-myc and anti-HA antibodies and analyzed by confocal laser microscopy. Scale bars = 10 μm. (C) Plasmids expressing Cardif or truncated Cardif (Cardif1-508) and pIFN-β-Fluc and pRL-CMV were transfected with or without plasmid expressing NS3/4A or NS4B into HEK293T cells as indicated. Dual luciferase assays were performed 24 hours after transfection. Plasmid expressing ΔCARD or pcDNA was used as a negative control. The *y* axis indicates IFN-β-Fluc activity shown as relative values. Assays were performed in triplicate, and error bars indicate the mean $\pm$ SD. $^*P < 0.05$.

HCV NS3/4A serine protease cleaves Cardif between Cys-508 and His-509, releases Cardif from the mitochondrial membrane, and blocks RIG-I–induced IFN-β production. We next assessed whether NS4B suppresses IFN-β production in the presence of Cardif cleaved by NS3/4A protease (Cardif1-508, Fig. 8A). The truncation of Cardif–C-terminal residue abolished mitochondrial localization but still colocalized with STING (Fig. 8B). The reporter assay showed that Cardif1-508 induced weak IFN-β activation. Interestingly, NS4B completely blocked the residual function of the Cardif1-508 protein to activate IFN-β expression, suggesting an additive effect of NS3/4A and NS4B on the RIG-I–activating pathway (Fig. 8C).

Discussion

It has been reported that viruses, including HCV, target IFN signaling to establish persistent replication in host cells.[39] We have reported that NS4B blocks the transcriptional activation of ISRE induced by overexpression of RIG-I and Cardif, but not by TBK1 or IKKϵ.[19] In the present study, we have shown that NS4B directly and specifically binds STING, an ER-residing scaffolding protein of Cardif and TBK1 and an inducer of IFN-β production (Figs. 3 and 5), and blocked the interaction between STING and Cardif (Fig. 5B,D) resulting in strong suppression of RIG-I–mediated phosphorylation of IRF-3 and expressional induction of IFN-β (Fig. 1). Furthermore, HCV replication was increased by knockdown of STING or overexpression of NS4B (Fig. 6). Taken together, our results demonstrate that HCV-NS4B strongly blocks virus-induced, RIG-I–mediated activation of IFN-β production signaling through targeting STING, which constitutes a novel mechanism of viral evasion from innate immune responses and establishment of persistent viral replication.

Our results also showed that the effects of NS4B on the RIG-I signaling were independent of NS3/4A-mediated cleavage of Cardif. Reporter assays showed that a cleaved form of Cardif (Cardif1-508) partially retained activity for the induction of IFN-β promoter activation. The residual IFN-β promoter activation was suppressed almost completely by NS4B but not by NS3/4A (Fig. 8C). These findings show that there are at least two mechanisms by which HCV can abrogate RIG-I–mediated IFN production signaling to accomplish abrogation of cellular antiviral responses.

NS4B and STING are ER proteins,[20,21,40] whereas Cardif is localized on the outer mitochondrial membrane.[9] Consistent with those reports, our immunostaining experiments demonstrated that most NS4B protein colocalized with STING (Fig. 2), and their association was localized on MAM (Fig. 2E). In addition to the significant colocalization of STING and NS4B, STING partially colocalized with Cardif at the boundary region of the two proteins (Fig. 2B). Furthermore, immunoprecipitation experiments showed that overexpression of NS4B completely blocked the interaction of STING with Cardif (Fig. 5B). Ishikawa et al.[24] reported

that STING could associate with Cardif by MAM interaction. Castanier et al.[41] reported that Cardif-STING interaction was enhanced in cells with elongated mitochondria. In addition, Horner et al.[42,43] observed NS3/4A targeting of MAM-anchored synapse and cleavage of Cardif at MAM but not in mitochondria. These results led us to speculate that interaction between STING and Cardif was enhanced by altering their subcellular localization during viral infection and that NS4B inhibits Cardif activation by interfering with the association between STING and Cardif on MAM-like NS3/4A behavior against host innate immunity.

HCV-NS4B is an ER-localized 27-kDa protein with several functions in the HCV life cycle. Cellular expression of NS4B induces convolution of the ER membrane and formation of a membranous web that harbors HCV replicase complex.[44,45] NS4B also has RNA-binding capacity.[46] In addition, several point mutations of NS4B were found to alter viral replication activity.[33,46,47] The studies above indicate that NS4B provides an important protein-protein or protein-RNA interaction platform within the HCV replication complex and is essential for viral RNA replication. However, there are few reports on the involvement of NS4B with antiviral immune responses. Consistent with our previous study, Moriyama et al.[48] reported that NS4B partially inhibited dsRNA-induced but not TRIF-induced activation of IFN-β. In NS4B-expressing cells, IFN-α induced activation of STAT1 was suppressed.[49] The present study has demonstrated that NS4B functions against the host IFN response, such that NS4B directly interacts with STING and suppresses downstream signaling, resulting in the induction of IFN production.

STING contains a domain homologous to the N terminus of NS4B derived from several flaviviruses, including HCV. In our previous NS4B truncation assay, the NS4B N-terminal domain (amino acids 1-110) was important for suppression of RIG-I–induced IFN-β expression.[19] Consistent with these results, N-terminally truncated NS4B (NS4Bt1-84) significantly suppressed STING and Cardif-induced IFN-β promoter activation, whereas the C terminus of NS4B (NS4Bt85-261) did not (Fig. 7). These results reinforce our hypothesis that NS4B binds STING at its homology domain and blocks the ability of STING to induce IFN-β production.

A small molecule inhibitor of NS4B has been developed and is under preliminary clinical trials.[50] Einav et al.[51] identified clemizole hydrochloride, an H1 histamine receptor antagonist, as an inhibitor of the RNA-binding function of NS4B and HCV RNA replication. A phase 1B clinical trial of clemizole in hepatitis C patients has been completed.[52] Other two NS4B inhibitors which are a compound of amiloride analog and anguizole are under preclinical development.[53,54] The possibility remains that such NS4B inhibitors may suppress HCV replication partly through inhibiting the ability of NS4B to suppress IFN-β production and restore cellular antiviral responses.

In conclusion, IFN production signaling induced by HCV infection and mediated by RIG-I is suppressed by NS4B through a direct interaction with STING. These virus-host interactions help to elucidate the mechanisms of persistent HCV infection and constitute a potential target to block HCV infection.

Acknowledgment: The authors are indebted to J. Tcshopp for providing Cardif, ΔCARD, and CARD and to G. N. Barber for the STING plasmids. This study was supported by grants from the Ministry of Education, Culture, Sports, Science and Technology, Japan; the Japan Society for the Promotion of Science; Ministry of Health, Labour and Welfare, Japan; and the Japan Health Sciences Foundation.

References

1. Samuel CE. Antiviral actions of interferons. Clin Microbiol Rev 2001; 14:778-809.
2. Taniguchi T, Takaoka A. The interferon-alpha/beta system in antiviral responses: a multimodal machinery of gene regulation by the IRF family of transcription factors. Curr Opin Immunol 2002;14:111-116.
3. Sakamoto N, Watanabe M. New therapeutic approaches to hepatitis C virus. J Gastroenterol 2009;44:643-649.
4. Bigger CB, Brasky KM, Lanford RE. DNA microarray analysis of chimpanzee liver during acute resolving hepatitis C virus infection. J Virol 2001;75:7059-7066.
5. Yoneyama M, Kikuchi M, Natsukawa T, Shinobu N, Imaizumi T, Miyagishi M, et al. The RNA helicase RIG-I has an essential function in duoble-stranded RNA-induced innate antiviral responses. Nat Immunol 2004;5:730-737.
6. Hornung V, Ellegast J, Kim S, Brzozka K, Jung A, Kato H, et al. 5'-Triphosphate RNA is the ligand for RIG-I. Science 2006;314:994-997.
7. Takahasi K, Yoneyama M, Nishihori T, Hirai R, Kumeta H, Narita R, et al. Nonself RNA-sensing mechanism of RIG-I helicase and activation of antiviral immune responses. Mol Cell 2008;29:428-440.
8. Kawai T. IPS-1, an adaptor triggering RIG-I- and Mda5-mediated type I interferon induction. Nat Immunol 2005;6:981-988.
9. Seth RB, Sun L, Ea CK, Chen ZJ. Identification and characterization of MAVS, a mitochondrial antiviral signaling protein that activates NF-κB and IRF 3. Cell 2005;122:669-682.
10. Xu LG. VISA is an adapter protein required for virus-triggered IFN-β signaling. Mol Cell 2005;19:727-740.
11. Meylan E, Curran J, Hofmann K, Moradpour D, Binder M, Bartenschlager R, et al. Cardif is an adaptor protein in the RIG-I antiviral pathway and is targeted by hepatitis C virus. Nature 2005;437: 1167-1172.
12. Yoneyama M, Suhara W, Fukuhara Y, Fukuda M, Nishida E, Fujita T. Direct triggering of the type I interferon system by virus infection: activation of a transcription factor complex containing IRF-3 and CBP/p300. EMBO J 1998;17:1087-1095.

13. Lin W, Kim SS, Yeung E, Kamegaya Y, Blackard JT, Kim KA, et al. Hepatitis C virus core protein blocks interferon signaling by interaction with the STAT1 SH2 domain. J Virol 2006;80:9226-9235.
14. Suda G, Sakamoto N, Itsui Y, Nakagawa M, Tasaka-Fujita M, Funaoka Y, et al. IL-6-mediated intersubgenotypic variation of interferon sensitivity in hepatitis C virus genotype 2a/2b chimeric clones. Virology 2010;407:80-90.
15. Funaoka Y, Sakamoto N, Suda G, Itsui Y, Nakagawa M, Kakinuma S, et al. Analysis of interferon signaling by infectious hepatitis C virus clones with substitutions of core amino acids 70 and 91. J Virol 2011; 85:5986-5994.
16. Loo YM, Owen DM, Li K, Erickson AK, Johnson CL, Fish PM, et al. Viral and therapeutic control of IFN-beta promoter stimulator 1 during hepatitis C virus infection. Proc Natl Acad Sci U S A 2006;103:6001-6006.
17. Li X-D, Sun L, Seth RB, Pineda G, Chen ZJ. Hepatitis C virus protease NS3/4A cleaves mitochondrial antiviral signaling protein off the mitochondria to evade innate immunity. Proc Natl Acad Sci U S A 2005; 102:17717-17722.
18. Baril M, Racine M-E, Penin F, Lamarre D. MAVS Dimer Is a Crucial Signaling Component of Innate Immunity and the Target of Hepatitis C Virus NS3/4A Protease. J. Virol. 2009;83:1299-1311.
19. Tasaka M, Sakamoto N, Itakura Y, Nakagawa M, Itsui Y, Sekine-Osajima Y, et al. Hepatitis C virus non-structural proteins responsible for suppression of the RIG-I/Cardif-induced interferon response. J Gen Virol 2007;88:3323-3333.
20. Ishikawa H, Barber GN. STING is an endoplasmic reticulum adaptor that facilitates innate immune signalling. Nature 2008;455:674-678.
21. Sun W, Li Y, Chen L, Chen H, You F, Zhou X, et al. ERIS, an endoplasmic reticulum IFN stimulator, activates innate immune signaling through dimerization. Proc Natl Acad Sci U S A 2009;106:8653-8658.
22. Zhong B, Yang Y, Li S, Wang YY, Li Y, Diao F, et al. The adaptor protein MITA links virus-sensing receptors to IRF3 transcription factor activation. Immunity 2008;29:538-550.
23. Jin L. MPYS, a novel membrane tetraspanner, is associated with major histocompatibility complex class II and mediates transduction of apoptotic signals. Mol Cell Biol 2008;28:5014-5026.
24. Ishikawa H, Ma Z, Barber GN. STING regulates intracellular DNA-mediated, type I interferon-dependent innate immunity. Nature 2009; 461:788-792.
25. Yanagi M, Purcell RH, Emerson SU, Bukh J. Transcripts from a single full-length cDNA clone of hepatitis C virus are infectious when directly trasfected into the liver of a chimpanzee. Proc Natl Acad Sci U S A 1997;94:8738-8743.
26. Lin R, Lacoste J, Nakhaei P, Sun Q, Yang L, Paz S, et al. Dissociation of a MAVS/IPS-1/VISA/Cardif-IKKepsilon molecular complex from the mitochondrial outer membrane by hepatitis C virus NS3-4A proteolytic cleavage. J Virol 2006;80:6072-6083.
27. Yokota T, Sakamoto N, Enomoto N, Tanabe Y, Miyagishi M, Maekawa S, et al. Inhibition of intracellular hepatitis C virus replication by synthetic and vector-derived small interfering RNAs. EMBO Rep 2003;4:602-608.
28. Tanabe Y, Sakamoto N, Enomoto N, Kurosaki M, Ueda E, Maekawa S, et al. Synergistic inhibition of intracellular hepatitis C virus replication by combination of ribavirin and interferon- alpha. J Infect Dis 2004;189:1129-1139.
29. Wakita T, Pietschmann T, Kato T, Date T, Miyamoto M, Zhao Z, et al. Production of infectious hepatitis C virus in tissue culture from a cloned viral genome. Nat Med 2005;11:791-796.
30. Lindenbach BD, Evans MJ, Syder AJ, Wolk B, Tellinghuisen TL, Liu CC, et al. Complete replication of hepatitis C virus in cell culture. Science 2005;309:623-626.
31. Nakagawa M, Sakamoto N, Enomoto N, Tanabe Y, Kanazawa N, Koyama T, et al. Specific inhibition of hepatitis C virus replication by cyclosporin A. Biochem Biophys Res Commun 2004;313:42-47.
32. Yamashiro T, Sakamoto N, Kurosaki M, Kanazawa N, Tanabe Y, Nakagawa M, et al. Negative regulation of intracellular hepatitis C virus replication by interferon regulatory factor 3. J Gastroenterol 2006;41:750-757.
33. Lindstrom H, Lundin M, Haggstrom S, Persson MA. Mutations of the hepatitis C virus protein NS4B on either side of the ER membrane affect the efficiency of subgenomic replicons. Virus Res 2006;121: 169-178.
34. Hayashi T, Rizzuto R, Hajnoczky G, Su TP. MAM: more than just a housekeeper. Trends Cell Biol 2009;19:81-88.
35. Lewin TM, Van Horn CG, Krisans SK, Coleman RA. Rat liver acyl-CoA synthetase 4 is a peripheral-membrane protein located in two distinct subcellular organelles, peroxisomes, and mitochondrial-associated membrane. Arch Biochem Biophys 2002;404:263-270.
36. Simmen T, Aslan JE, Blagoveshchenskaya AD, Thomas L, Wan L, Xiang Y, et al. PACS-2 controls endoplasmic reticulum-mitochondria communication and Bid-mediated apoptosis. EMBO J 2005;24:717-729.
37. Kerppola TK. Design and implementation of bimolecular fluorescence complementation (BiFC) assays for the visualization of protein interactions in living cells. Nat Protoc 2006;1:1278-1286.
38. Kerppola TK. Bimolecular fluorescence complementation (BiFC) analysis as a probe of protein interactions in living cells. Annu Rev Biophys 2008;37:465-487.
39. Kato H. Differential roles of MDA5 and RIG-I helicases in the recognition of RNA viruses. Nature 2006;441:101-105.
40. Saitoh T, Fujita N, Hayashi T, Takahara K, Satoh T, Lee H, et al. Atg9a controls dsDNA-driven dynamic translocation of STING and the innate immune response. Proc Natl Acad Sci U S A 2009;106: 20842-20846.
41. Castanier C, Garcin D, Vazquez A, Arnoult D. Mitochondrial dynamics regulate the RIG-I-like receptor antiviral pathway. EMBO Rep 2009;11:133-138.
42. Horner SM, Liu HM, Park HS, Briley J, Gale M. Mitochondrial-associated endoplasmic reticulum membranes (MAM) form innate immune synapses and are targeted by hepatitis C virus. Proc Natl Acad Sci U S A 2011;108:14590-14595.
43. Horner SM, Park HS, Gale M Jr. Control of innate immune signaling and membrane targeting by the hepatitis C virus NS3/4A protease are governed by the NS3 helix α0. J Virol 2012;86:3112-3120.
44. Egger D, Wolk B, Gosert R, Bianchi L, Blum HE, Moradpour D, et al. Expression of Hepatitis C virus proteins induces distinct membrane alterations including a candidate viral replication complex. J Virol 2002;76:5974-5984.
45. Gretton SN, Taylor AI, McLauchlan J. Mobility of the hepatitis C virus NS4B protein on the endoplasmic reticulum membrane and membrane-associated foci. J Gen Virol 2005;86:1415-1421.
46. Einav S, Elazar M, Danieli T, Glenn JS. A nucleotide binding motif in hepatitis C virus (HCV) NS4B mediates HCV RNA replication. J Virol 2004;78:11288-11295.
47. Elazar M, Liu P, Rice CM, Glenn JS. An N-terminal amphipathic helix in hepatitis C virus (HCV) NS4B mediates membrane association, correct localization of replication complex proteins, and HCV RNA replication. J Virol 2004;78:11393-11400.
48. Moriyama M, Kato N, Otsuka M, Shao RX, Taniguchi H, Kawabe T, et al. Interferon-beta is activated by hepatitis C virus NS5B and inhibited by NS4A, NS4B, and NS5A. Hepatol Int 2007;1:302-310.
49. Xu J, Liu S, Xu Y, Tien P, Gao G. Identification of the nonstructural protein 4B of hepatitis C virus as a factor that inhibits the antiviral activity of interferon-alpha. Virus Res 2009;141:55-62.
50. Hofmann WP, Zeuzem S. A new standard of care for the treatment of chronic HCV infection. Nat Rev Gastroenterol Hepatol 2011;8: 257-264.
51. Einav S, Gerber D, Bryson PD, Sklan EH, Elazar M, Maerkl SJ, et al. Discovery of a hepatitis C target and its pharmacological inhibitors by microfluidic affinity analysis. Nat Biotech 2008;26:1019-1027.
52. Rai R, Deval J. New opportunities in anti-hepatitis C virus drug discovery: targeting NS4B. Antiviral Res 2011;90:93-101.
53. Cho NJ, Dvory-Sobol H, Lee C, Cho SJ, Bryson P, Masek M, et al. Identification of a class of HCV inhibitors directed against the nonstructural protein NS4B. Sci Transl Med 2010;2:15ra16.
54. Bryson PD, Cho NJ, Einav S, Lee C, Tai V, Bechtel J, et al. A small molecule inhibits HCV replication and alters NS4B's subcellular distribution. Antiviral Res 2010;87:1-8.

JOURNAL OF VIRAL HEPATITIS

Journal of Viral Hepatitis, 2013, **20**, 72–76 doi:10.1111/j.1365-2893.2012.01635.x

Noninvasive estimation of fibrosis progression overtime using the FIB-4 index in chronic hepatitis C

N. Tamaki, M. Kurosaki, K. Tanaka, Y. Suzuki, Y. Hoshioka, T. Kato, Y. Yasui, T. Hosokawa, K. Ueda, K. Tsuchiya, H. Nakanishi, J. Itakura, Y. Asahina and N. Izumi *Division of Gastroenterology and Hepatology, Musashino Red Cross Hospital, Tokyo, Japan*

Received February 2012; accepted for publication May 2012

SUMMARY. The FIB-4 index is a simple formula to predict liver fibrosis based on the standard biochemical values (AST, ALT and platelet count) and age. We here investigated the utility of the index for noninvasive prediction of progression in liver fibrosis. The time-course alteration in the liver fibrosis stage between paired liver biopsies and the FIB-4 index was examined in 314 patients with chronic hepatitis C. The average interval between liver biopsies was 4.9 years. The cases that showed a time-course improvement in the fibrosis stage exhibited a decrease in the FIB-4 index, and those that showed deterioration in the fibrosis stage exhibited an increase in the FIB-4 index with a significant correlation ($P < 0.001$). Increase in the ΔFIB-4 index per year was an independent predictive factor for the progression in liver fibrosis with an odds ratio of 3.90 ($P = 0.03$). The area under the receiver operating characteristic curve of the ΔFIB-4 index/year for the prediction of advancement to cirrhosis was 0.910. Using a cut-off value of the ΔFIB-4 index/year <0.4 or ≥0.4, the cumulative incidence of fibrosis progression to cirrhosis at 5 and 10 years was 34% and 59%, respectively in patients with the ΔFIB-4 index/year ≥0.4, whereas it was 0% and 3% in those with the ΔFIB-4 index/year <0.4 ($P < 0.001$). In conclusion, measurement of the time-course changes in the FIB-4 index is useful for the noninvasive and real-time estimation of the progression in liver fibrosis.

Keywords: FIB-4, fibrosis, HCV, noninvasive.

INTRODUCTION

Advanced stage of liver fibrosis in chronic hepatitis C is associated with failure of interferon therapy or development of major concomitant disease such as variceal bleeding, liver failure and hepatocellular carcinoma [1–3]. Therefore, evaluation of the stage of liver fibrosis is essential in clinical practice. Liver biopsy is the gold standard for diagnosis of liver fibrosis [4,5], but inaccuracy in evaluation of fibrosis because of sampling errors [6–8] or by the inter-observer variation has been reported [9]. Real-time assessment of liver fibrosis may be clinically useful, but the invasiveness of liver biopsy precludes repeated examinations.

A variety of noninvasive methods to diagnose liver fibrosis have been proposed. Recently, transient elastography [10–13] and real-time tissue elastography [14] using ultrasonography have been developed, but these modalities are not widely available. For blood tests, the aspartate aminotransferase (AST)/alanine aminotransferase (ALT) ratio [15], the AST/platelet ratio index (APRI) [16,17] and the Fibrotest [18,19] have been reported to be useful. The FIB-4 index is another prediction value of liver fibrosis in chronic hepatitis C based on the standard biochemical values and age. The FIB-4 index has been reported to be markedly useful for the prediction of advanced liver fibrosis [20,21]. Given its noninvasiveness and simplicity, the FIB-4 index has the advantage of an easy follow-up of the time-course changes by repeated measurements.

In the present study, we investigated the utility of the real-time assessment of the FIB-4 index for the prediction of time-course progression in liver fibrosis.

Abbreviations: ALT, alanine aminotransferase; AST, aspirate aminotransferase; HBV, hepatitis B virus; HCV, hepatitis C virus; HIV, human immunodeficiency virus.

Correspondence: Namiki Izumi, MD, Division of Gastroenterology and Hepatology, Musashino Red Cross Hospital, 1-26-1 Kyonan-cho, Musashino-shi, Tokyo 180-8610, Japan. E-mail: nizumi@musashino.jrc.or.jp

PATIENTS AND METHODS

Patients

A total of 421 patients with chronic hepatitis C who had repeated liver biopsies between 1991 and 2010 at the Musashino Red Cross hospital were consecutively investigated. All patients received interferon therapy after the first biopsy and had nonsustained virological response. A second

biopsy was performed at least 6 months after the completion of interferon therapy. Exclusion criteria were as follows: (i) co-infection with HBV or HIV (n = 1), (ii) alcohol abuse (intake of alcohol equivalent to pure alcohol 40 g/day or more) (n = 8), (iii) the presence of nonalcoholic steatohepatitis (n = 14), (iv) the presence of hepatocellular carcinoma (n = 15), (v) interval between paired biopsies was <1.5 years (n = 41) and (vi) length of biopsy sample <15 mm (n = 28). The demographic characteristics of the 314 patients enrolled are shown in Table 1.

Assessment of liver fibrosis stage

Liver biopsy was carried out under laparoscopic or ultrasonographic guidance. A sample 15 mm or larger was collected and evaluated. The fibrosis stage was categorized according to the METAVIR score: F0, no fibrosis; F1, portal fibrosis without septa; F2, portal fibrosis with few septa; F3, numerous septa without cirrhosis; and F4, cirrhosis. Two pathologists examined all samples and determined the fibrosis stage. When staging was inconsistent between the two pathologists, an appropriate stage was determined by discussion between the two.

Calculation of FIB-4 index

The FIB-4 index at the time of each liver biopsy was calculated based on the blood test results within 1 month before liver biopsy according to the following formula: The FIB-4 index = (age [years] × AST [IU/L])/(platelet count [10^9/L] × (ALT [IU/L])$^{1/2}$). Change in the FIB-4 index per year (ΔFIB-4 index/year) was calculated by the following formula: ΔFIB-4 index/year = (the FIB-4 index at the second liver biopsy − the FIB-4 index at the first liver biopsy)/interval between paired biopsies (years). Change in AST, ALT, platelet counts per year (ΔAST/year, ΔALT/year, ΔPlatelet counts/year) and the degree of changes in the fibrosis stage per year were calculated similarly.

Table 1 Clinical background of patients

	First biopsy	Second biopsy
Age (years)	53.7 ± 9.8	58.7 ± 9.4
Gender (male/female)	149/165	
AST (IU/L)	64.5 ± 36.7	58.5 ± 37.7
ALT (IU/L)	87.7 ± 58.9	69.9 ± 53.9
Platelet counts (× 10^9/L)	165 ± 48	159 ± 48
Histological findings		
Activity: 0/1/2/3	38/143/117/16	10/147/131/26
Fibrosis: 0–1/2/3/4	139/107/61/7	134/101/63/16
Interval of between biopsies (years)	4.9 ± 2.9	–

AST, aspartate aminotransferase; ALT, alanine aminotransferase.

Statistical analysis

The SPSS software package 15.0 (SPSS Inc, Chicago, IL, USA) was used for statistical analysis. Categorical data were analysed using Fisher's exact test. Continuous variables were compared with Student's t-test. Factors associated with the progression in liver fibrosis were analysed by multivariate logistic regression analysis. Association between progression in fibrosis stage and changes in the FIB-4 was analysed by Spearman's rank correlation test. Kaplan–Meier method and log-rank test were used to analyse time to occurrence of fibrosis progression to cirrhosis. A P-value of < 0.05 was considered statistically significant.

RESULTS

Changes in liver fibrosis stage overtime

The clinical backgrounds of patients at the first and second biopsies are shown in Table 1. The average interval was 4.9 years between the two liver biopsies. The fibrosis stage progressed over time in 23%, regressed in 17% and remained unchanged in 60%. Changes of fibrosis stage stratified by the fibrosis stage at the first liver biopsy are shown in Table 2.

Comparison of FIB-4 index and liver fibrosis stage

For the prediction of advanced liver fibrosis (F3–4), a FIB-4 index <1.45 had a negative predictive value of 97%, whereas a FIB-4 > 3.25 had a positive predictive value of 49% at first biopsy. Similarly, a FIB-4 < 1.45 had a negative predictive value of 98%, and a FIB-4 > 3.25 had a positive predictive value of 54% at second biopsy (Fig. 1).

Table 2 Changes of fibrosis stage over time

	Fibrosis stage at second biopsy				
Fibrosis stage at first biopsy	F0–1 (%)	F2 (%)	F3 (%)	F4 (%)	Total
F0–1	98 (71)	33 (24)	8 (5)	–	139
F2	33 (31)	50 (47)	21 (20)	3 (2)	107
F3	3 (5)	18 (29)	33 (55)	7 (11)	61
F4	–	–	1 (14)	6 (86)	7

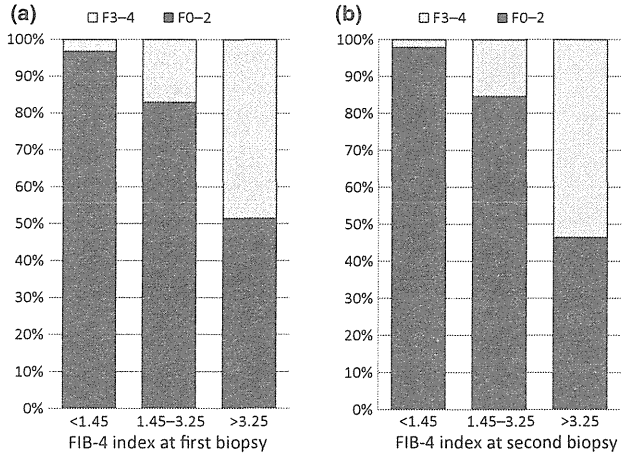

Fig. 1 Comparison of the FIB-4 index and liver fibrosis stage. Patients were categorized into three groups according to the FIB-4 index using cut-off values of < 1.45, 1.45–3.25, > 3.25 at liver biopsy. The lower bar chart (dark grey) indicates patients with F0–2, while the upper bar chart (light grey) indicates patients with F3–4. (a) comparison of the FIB-4 index and liver fibrosis stage at first biopsy and (b) at second biopsy.

Predictive factors for the progression of fibrosis

Higher level of ΔAST/year, lower level of ΔALT/year, lower level of ΔPlatelet counts/year and higher level of the ΔFIB-4/year were significantly associated with the progression of fibrosis overtime (Table 3). Multivariate analysis demonstrated that only the ΔFIB-4 index/year was an independent predictive factor for the progression of fibrosis stage ($P = 0.03$) with an odds ratio of 3.70 (95% CI:1.07–12.5).

Correlation between the degree of changes in the fibrosis stage and the ΔFIB-4 index per year

When the patients were categorized into five groups according to the degree of changes in the fibrosis stage per year (< −0.2, −0.2 – < 0, 0, > 0 – 0.2 and > 0.2), median value of the ΔFIB-4 index/year was −0.29, −0.02, 0.04, 0.16 and 0.47, respectively. The FIB-4 index reduced along the regression of the fibrosis stage, while the FIB-4 index increased along the progression of the fibrosis stage, which showed a significant correlation ($P < 0.001$) (Fig. 2).

Prediction of progression to cirrhosis by the changes in the FIB-4 index per year

The area under the receiver operating characteristic curve of the ΔFIB-4 index/year for the prediction of advancement to cirrhosis was 0.910. By the ΔFIB-4 index/year of 0.4, the sensitivity and specificity for the prediction of advancement to cirrhosis was 80% and 91%. The cumulative incidence of fibrosis progression to cirrhosis, at 5 and 10 years, was 34% and 59%, respectively, in patients with the ΔFIB-4 index/year ≥0.4, whereas it was 0% and 3% in those with the ΔFIB-4 index/year <0.4 ($P < 0.001$) (Fig. 3).

DISCUSSION

Recently, noninvasive markers of liver fibrosis have been used as a predictive factor of liver-related outcome such as

Table 3 Factors associated with the progression of liver fibrosis

	Progression of Liver fibrosis	Nonprogression of Liver fibrosis	*P*-value
Gender (male/female)	31/42	118/123	0.33
Age at first biopsy (years)	54.4 ± 8.7	53.5 ± 10.2	0.50
AST at first biopsy (IU/L)	63.9 ± 35.0	64.8 ± 37.3	0.85
ALT at first biopsy (IU/L)	86.5 ± 58.4	88.1 ± 59.2	0.84
Platelet counts at first biopsy (10^9/L)	15.8 ± 4.6	16.7 ± 4.8	0.16
Change between biopsies			
ΔAST (IU/L)/year	3.8 ± 19.5	−4.1 ± 14.8	<0.001
ΔALT (IU/L)/year	−1.9 ± 28.4	7.2 ± 22.6	0.005
ΔPlatelet counts (10^9/L)/year	−4.1 ± 9.5	−0.002 ± 9.5	0.001
ΔFIB-4 index/year	0.31 ± 0.52	−0.005 ± 0.37	<0.001

ΔAST/year: (AST at the second liver biopsy – AST at the first liver biopsy) /interval between paired biopsies (years); ΔALT/year: (ALT at the second liver biopsy – ALT at the first liver biopsy) /interval between paired biopsies (years); ΔPlatelet counts/year: (platelet counts at the second liver biopsy –platelet counts at the first liver biopsy) /interval between paired biopsies (years); ΔFIB-4 index /year: (the FIB-4 index at the second liver biopsy – the FIB-4 index at the first liver biopsy) /interval between paired biopsies (years).

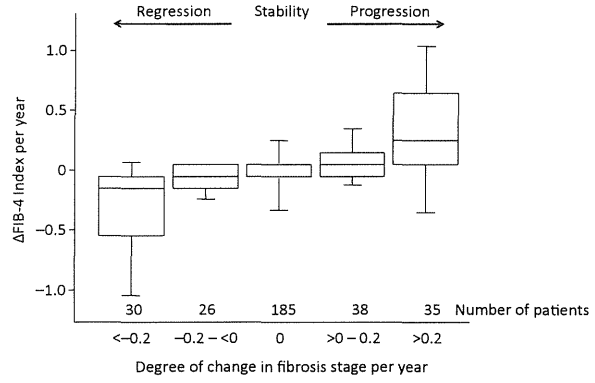

Fig. 2 Correlation between the degree of changes in the fibrosis stage and the ΔFIB-4 index per year. Boxplot of the ΔFIB-4 index/year is shown according to the degree of changes in the fibrosis stage per year. The bottom and top of each box represent the 25 and 75th percentiles, giving the interquartile range. The line through the box indicates the median value, and the error bar indicates the 5 and 95th percentiles.

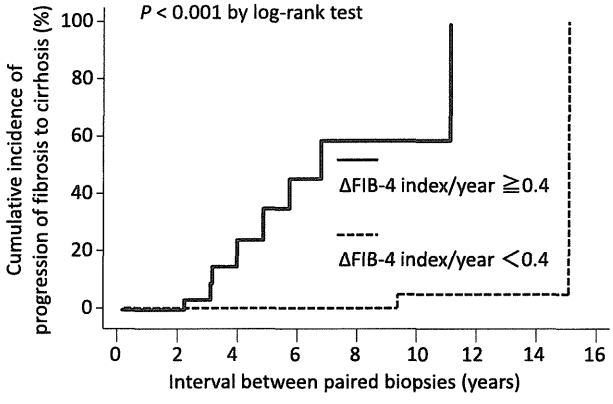

Fig. 3 Cumulative incidence of fibrosis progression to cirrhosis. Patients were categorized into two groups according to the ΔFIB-4 index/year using cut-off value of < 0.4 or ≥ 0.4.

mortality [22–24] or HCC development [24–26] in patients with chronic liver disease. There have been few studies that investigated the association between changes of noninvasive markers and liver-related outcome [27–29]. However, it is still unclear whether there is a relation between the time-course changes in the value of noninvasive markers and progression of liver fibrosis.

The aim of the study was to evaluate the utility of the real-time assessment of the FIB-4 index for the prediction of time-course progression in liver fibrosis. We have shown that the FIB-4 index reduced along the regression of the fibrosis stage, while the FIB-4 index increased along the progression of the fibrosis stage. These results indicate that the measurement of the time-course changes in the FIB-4 index may be useful for the noninvasive and real-time estimation of the progression in liver fibrosis overtime.

Although the gold standard for diagnosis of liver fibrosis is liver biopsy, there are a variety of problems including invasiveness and sampling errors [6]. Diagnostic methods of liver fibrosis by measurement of elasticity of the liver by ultrasonography [10–14] have been developed, but these modalities are not widely available.

The FIB-4 index has an advantage among these noninvasive liver fibrosis diagnostic methods. Firstly, it is quite easily calculated. The parameters required for calculation are only age, AST, ALT and platelet counts, which are measured at the routine examination of patients with liver disease. Therefore, additional blood collection is unnecessary, and the index can be calculated at no cost. Secondly, because of its simple calculation, it is possible to evaluate the clinical conditions in a real-time manner. Repeated measurements of the FIB-4 index make it possible to predict deterioration in liver fibrosis continuously over time. Because no special equipment or system is necessary, and objective data on the clinical conditions are provided in a real-time manner, the FIB-4 index is simple and convenient compared with other noninvasive liver fibrosis diagnostic methods.

It is widely known that a decrease in platelet counts is useful for the prediction of the progression of fibrosis stage [30]. We have reported that elevated AST or ALT is also associated with the progression of liver fibrosis [31]. However, the results of this study showed that a change in the FIB-4 index over time was a more useful factor for the prediction of the progression of fibrosis stage than AST, ALT and changes in platelet counts.

Liver biopsy is still an important examination as the gold standard for diagnosis of liver fibrosis, but time-course changes cannot be readily observed by repeated biopsies because of its invasiveness. On the other hand, it is possible to estimate the progression of liver fibrosis by repeated measurement of the FIB-4 index. Therefore, two examinations should be combined: liver biopsy may be utilized to determine the baseline of fibrosis stage, and the serial measurement of the FIB-4 index may be utilized to predict changes of fibrosis stages overtime in a real-time manner.

In conclusion, we believe that measurement of the time-course changes in the FIB-4 index is useful for the noninvasive and real-time estimation of the progression in liver fibrosis.

ACKNOWLEDGEMENTS

This study was supported by a grant-in-aid from Ministry of Health, Labor and Welfare, Japan.

CONFLICT OF INTEREST

No conflicts of interest exist for all authors.

REFERENCES

1 Dienstag JL. The role of liver biopsy in chronic hepatitis C. *Hepatology* 2002; 5(Suppl 1): S152–S160.
2 Benvegnu L, Gios M, Boccato S, Alberti A. Natural history of compensated viral cirrhosis: a prospective study on the incidence and hierarchy of major complications. *Gut* 2004; 53(5): 744–749.
3 Serfaty L, Aumaitre H, Chazouilleres O *et al.* Determinants of outcome of compensated hepatitis C virus-related cirrhosis. *Hepatology* 1998; 27(5): 1435–1440.
4 Gebo KA, Herlong HF, Torbenson MS *et al.* Role of liver biopsy in management of chronic hepatitis C: a systematic review. *Hepatology* 2002; 5(Suppl 1): S161–S172.
5 Saadeh S, Cammell G, Carey WD, Younossi Z, Barnes D, Easley K. The role of liver biopsy in chronic hepatitis C. *Hepatology* 2001; 33(1): 196–200.
6 Bravo AA, Sheth SG, Chopra S. Liver biopsy. *N Engl J Med* 2001; 344(7): 495–500.
7 Bedossa P, Dargere D, Paradis V. Sampling variability of liver fibrosis in chronic hepatitis C. *Hepatology* 2003; 38(6): 1449–1457.
8 Colloredo G, Guido M, Sonzogni A, Leandro G. Impact of liver biopsy size on histological evaluation of chronic viral hepatitis: the smaller the sample, the milder the disease. *J Hepatol* 2003; 39(2): 239–244.
9 The French METAVIR Cooperative Study Group. Intraobserver and interobserver variations in liver biopsy interpretation in patients with chronic hepatitis C. *Hepatology* 1994; 20(1 Pt 1): 15–20.
10 Sandrin L, Fourquet B, Hasquenoph JM *et al.* Transient elastography: a new noninvasive method for assessment of hepatic fibrosis. *Ultrasound Med Biol* 2003; 29(12): 1705–1713.
11 Ganne-Carrie N, Ziol M, de Ledinghen V *et al.* Accuracy of liver stiffness measurement for the diagnosis of cirrhosis in patients with chronic liver diseases. *Hepatology* 2006; 44(6): 1511–1517.
12 Foucher J, Chanteloup E, Vergniol J *et al.* Diagnosis of cirrhosis by transient elastography (FibroScan): a prospective study. *Gut* 2006; 55(3): 403–408.
13 Castera L, Vergniol J, Foucher J *et al.* Prospective comparison of transient elastography, Fibrotest, APRI, and liver biopsy for the assessment of fibrosis in chronic hepatitis C. *Gastroenterology* 2005; 128(2): 343–350.
14 Tatsumi C, Kudo M, Ueshima K *et al.* Noninvasive evaluation of hepatic fibrosis using serum fibrotic markers, transient elastography (FibroScan) and real-time tissue elastography. *Intervirology* 2008; 51(Suppl 1): 27–33.
15 Williams AL, Hoofnagle JH. Ratio of serum aspartate to alanine aminotransferase in chronic hepatitis. Relationship to cirrhosis. *Gastroenterology* 1988; 95(3): 734–739.
16 Wai CT, Greenson JK, Fontana RJ *et al.* A simple noninvasive index can predict both significant fibrosis and cirrhosis in patients with chronic hepatitis C. *Hepatology* 2003; 38(2): 518–526.
17 Lin ZH, Xin YN, Dong QJ *et al.* Performance of the aspartate aminotransferase-to-platelet ratio index for the staging of hepatitis C-related fibrosis: an updated meta-analysis. *Hepatology* 2011; 53(3): 726–736.
18 Imbert-Bismut F, Ratziu V, Pieroni L, Charlotte F, Benhamou Y, Poynard T. Biochemical markers of liver fibrosis in patients with hepatitis C virus infection: a prospective study. *Lancet* 2001; 357(9262): 1069–1075.
19 Sebastiani G, Vario A, Guido M *et al.* Stepwise combination algorithms of non-invasive markers to diagnose significant fibrosis in chronic hepatitis C. *J Hepatol* 2006; 44(4): 686–693.
20 Sterling RK, Lissen E, Clumeck N *et al.* Development of a simple noninvasive index to predict significant fibrosis in patients with HIV/HCV coinfection. *Hepatology* 2006; 43(6): 1317–1325.
21 Vallet-Pichard A, Mallet V, Nalpas B *et al.* FIB-4: An inexpensive and accurate marker of fibrosis in HCV infection. Comparison with liver biopsy and fibrotest. *Hepatology* 2007; 46(1): 32–36.
22 Vergniol J, Foucher J, Terrebonne E *et al.* Noninvasive tests for fibrosis and liver stiffness predict 5-year outcomes of patients with chronic hepatitis C. *Gastroenterology* 2011; 140(7): 1970–1979. 1979 e1971-1973.
23 Nunes D, Fleming C, Offner G *et al.* Noninvasive markers of liver fibrosis are highly predictive of liver-related death in a cohort of HCV-infected individuals with and without HIV infection. *Am J Gastroenterol* 2010; 105(6): 1346–1353.
24 Fung J, Lai CL, Seto WK, Wong DK, Yuen MF. Prognostic significance of liver stiffness for hepatocellular carcinoma and mortality in HBeAg-negative chronic hepatitis B. *J Viral Hepat* 2011; 18(10): 738–744.
25 Masuzaki R, Tateishi R, Yoshida H *et al.* Prospective risk assessment for hepatocellular carcinoma development in patients with chronic hepatitis C by transient elastography. *Hepatology* 2009; 49(6): 1954–1961.
26 Jung KS, Kim SU, Ahn SH *et al.* Risk assessment of hepatitis B virus-related hepatocellular carcinoma development using liver stiffness measurement (FibroScan). *Hepatology* 2011; 53(3): 885–894.
27 Vergniol J, Foucher J, Castera L *et al.* Changes of non-invasive markers and FibroScan values during HCV treatment. *J Viral Hepat* 2009; 16(2): 132–140.
28 Mummadi RR, Petersen JR, Xiao SY, Snyder N. Role of simple biomarkers in predicting fibrosis progression in HCV infection. *World J Gastroenterol* 2010; 16(45): 5710–5715.
29 Jain MK, Seremba E, Bhore R *et al.* Change in fibrosis score as a predictor of mortality among HIV-infected patients with viral hepatitis. *AIDS Patient Care STDS* 2012; 26(2): 73–80.
30 Poynard T, Bedossa P. Age and platelet count: a simple index for predicting the presence of histological lesions in patients with antibodies to hepatitis C virus. METAVIR and CLINIVIR Cooperative Study Groups. *J Viral Hepat* 1997; 4(3): 199–208.
31 Kurosaki M, Matsunaga K, Hirayama I *et al.* The presence of steatosis and elevation of alanine aminotransferase levels are associated with fibrosis progression in chronic hepatitis C with non-response to interferon therapy. *J Hepatol* 2008; 48(5): 736–742.

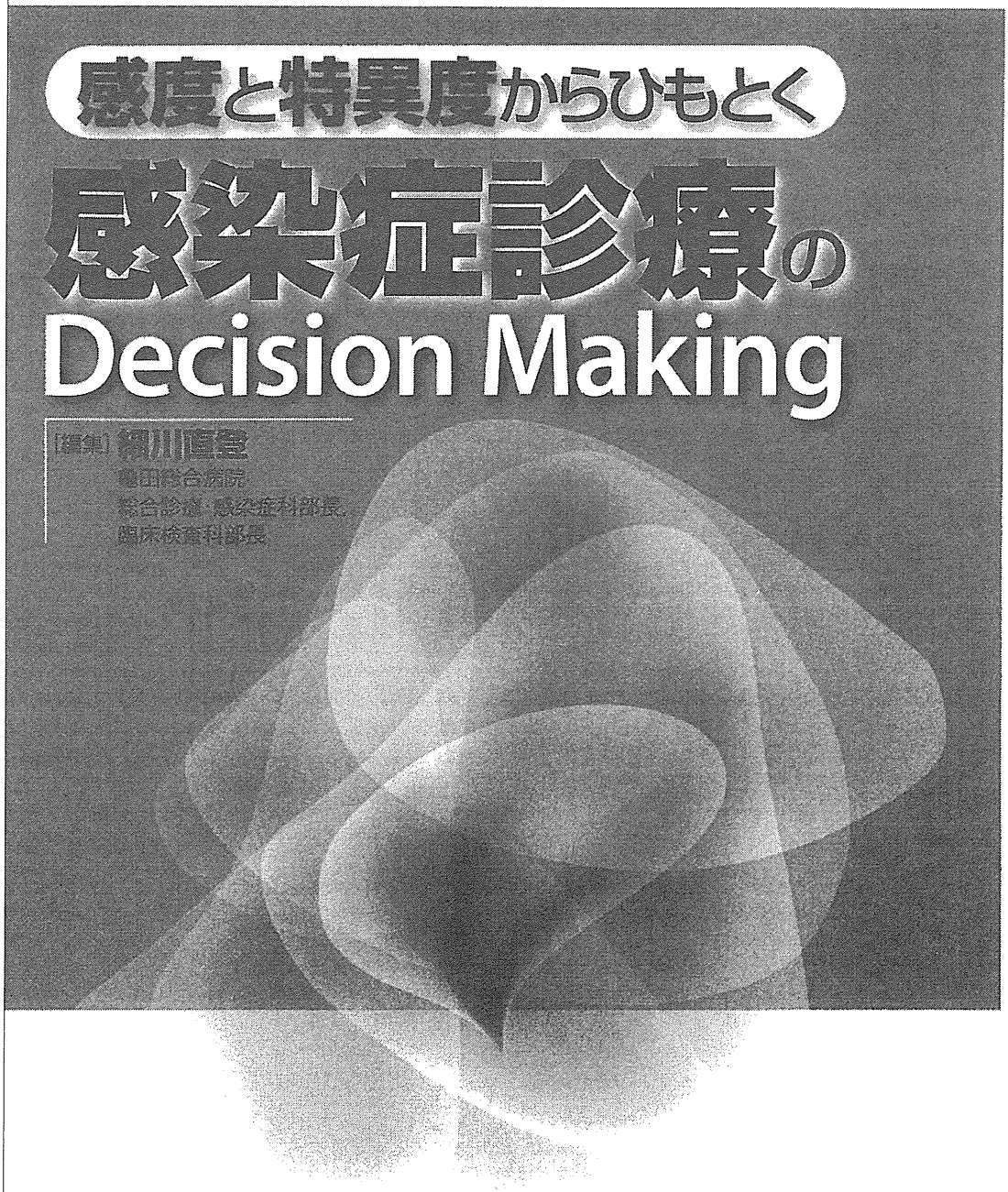
感度と特異度からひもとく
感染症診療の
Decision Making
[編集] 岩川直宏
豊田厚生病院
総合診療・感染症科部長、
臨床検査科部長

文光堂

3. 抗原・抗体検査 C. ウイルス

C型肝炎ウイルスマーカー

1 アウトライン

●C型肝炎の診断に用いられる検査

検査法	測定物質	検査目的
HCV抗体検査（第3世代）	HCVに感染した宿主が作る抗体を測定	・HCV感染状態のスクリーニング
HCVコア抗原	HCV粒子を構成するコア粒子の蛋白を直接測定	・HCV抗体低～中力価陽性者の二次検査 ・抗ウイルス療法の効果予測 ・抗ウイルス療法中のHCVモニタリング ・急性肝炎の迅速診断
核酸増幅検査	血中に微量に存在するHCVゲノム（HCV-RNA）をリアルタイムPCR法により増幅し測定	・HCVの最終的存在診断 ・抗ウイルス療法の効果予測 ・抗ウイルス療法中のHCVモニタリング

1. HCV抗体検査（第3世代）

現在認可を受けて市販されている各種のHCV抗体検査（第3世代）の試薬を用いた場合，真の意味での偽陽性反応と偽陰性反応はほとんどない．

C型肝炎ウイルス（HCV）は，直径55～57nmの球形をしたRNA型のウイルスで，ウイルスゲノムとこれを包んでいるヌクレオカプシド（コア粒子），およびこれを覆う外殻（エンベロープ）から成り立っている．HCVゲノムは，構造蛋白としてコア蛋白とエンベロープ蛋白（E1，E2/NS1）を，非構造蛋白としてNS2，NS3，NS4，NS5をコードしている．HCV抗体とは，HCVのコア粒子に対する抗体（HCVコア抗体），エンベロープに対する抗体（E2/NS-1抗体），非構造蛋白に対する抗体（NS抗体：C100-3抗体，C-33c抗体，NS5抗体など）のすべてを含む総称である．

HCV抗体検査は，HCV抗体測定系で用いられるHCV抗原の種類の世代により第1世代から第3世代まである．現在用いられている，第3世代HCV抗体検査はHCV感染診断のスクリーニングに用いられる．なお，これらHCV抗体は中和抗体ではないため，HCVに対する宿主の防御免疫を示すものではない．

2. HCVコア抗原検査

HCVのコア粒子の表面を構成する蛋白がHCVコア抗原である．HCVコア抗原は，エンベロープに覆われており HCV 粒子の内部に存在することと，血清中にはHCV コア抗体が多量に存在することから，HCV コア抗原の検出には HCV 粒子とコア抗体をペプチドに分解する前処理が必要である．検体（血清）を前処理した後に HCV のコア抗原を酵素抗体法（EIA 法）や免疫化学発光法などの手法を用いて検出する方法が HCV コア抗原の検査法である．本法は，簡便で安価である上，血清中の HCV の存在の有無を直接知ることができ，感度に優れ，コア抗原量はウイルス量と相関するため定量性がよい．単位はコア抗原量を分子数に換算したf（femto＝10^{-15}）molを用いる．1fmol/Lは約HCVゲノム100copy/mLと考えるとわかりやすい．HCVコア抗原検査は，①肝炎ウイルス検診（HCV抗体低～中力価陽性者の二次検査に使用），②インターフェロン療法の効果予測（高ウイルス量域まで測定可能），③抗ウイルス療法中の HCV モニタリング（ダイナミックレンジが広い），④急性肝炎の迅速診断（短時間で結果が得られる）において有用である．

3. 核酸増幅検査（HCV）

polymerase chain reaction（PCR）を用いて HCV の標的とするゲノムの一部を試験管内で約1億倍に増やして検出する方法で，検体（血清）の中に存在するごく微量のHCVゲノムすなわちHCV RNAをきわめて高感度に検出可能な方法である．現在はリアルタイム PCR 法が用いられており，HCV の検出法としては最も感度が高いため HCV の最終的存在診断として用いられる．また HCV は1粒子あたり1分子（1コピー）のHCV-RNAをゲノムとして内包しているため，リアルタイムPCR法を用いてHCV-RNAのコピー数を測定することでウイルス量が定量できる．本法はその感度のみならず定量性にも優れるため抗ウイルス療法を行う際の抗ウイルス効果の予測や，治療中の HCV モニターおよび最終的治療効果の判断に用いられる．

2 診断と見極めのポイント

1. HCV感染の診断

HCV感染の診断やスクリーニングには，通常まずHCV抗体検査を実施する．「HCV抗体陽性」は，「現在のHCVの感染（HCVキャリア）」または「過去のHCV感染の治癒（感染の既往）」を意味する．したがって，HCV感染の診断には両者を適

切に区別する必要があり，HCV抗体検査に加えHCVコア抗原検査や核酸増幅検査を組み合わせて判断する．

HCVキャリアでは，抗原刺激に常にさらされているため，HCV抗体は「高力価」陽性となることが多い．一方，C型急性肝炎の自然治癒例や，HCVキャリアであった人がインターフェロン治療などにより，HCVが体内から完全に排除されて治癒した症例では，年単位の経過でHCV抗体は「中力価」～「低力価」陽性へと低下する．ただし，抗体産生能力には個人差があることから，HCVキャリアでもHCV抗体「中力価」陽性や「低力価」陽性となることがある．

一般に，HCV抗体検査では，cut off index 1.0以上が陽性と判断される．高力価陽性（cut off index 50以上）の場合は，ほぼ100％ウイルス血症を認めるが，反対に4.0未満の低力価陽性の場合はウイルス血症を認めないことが多い．したがって，特に中・低抗体価（cut off index 50未満）の場合は，HCVコア抗原検査または核酸増幅検査を実施し，これらで陽性と判定されればHCV感染状態と診断する．ただし，HCVコア抗原検査と核酸増幅検査では後者の方が高感度であるため，HCVコア抗原検査で感度以下と判定された場合では，さらに核酸増幅検査でHCV-RNAの有無を判定する必要がある．

2. C型肝炎ウイルス検診

わが国では，C型肝炎ウイルス検診が行われており，肝炎検診で用いられている肝炎スクリーニング検査のアルゴリズムを図1に示す．一般に，下記に示す者はHCV感染の可能性が通常より高いと考えられるため，HCV検査を受けることが推奨されているが，これらのリスクを有しない人でもHCVキャリアであることが多いため注意を要する．

1) 平成4（1992）年以前に輸血を受けたことがある（出産時を含む）人
2) 長期に血液透析を受けている人
3) 輸入非加熱血液凝固因子製剤を投与されたことがある人
4) 3）と同等のリスクを有する非加熱凝固因子製剤を投与されたことがある人
5) フィブリノゲン製剤（フィブリン糊を含む）を投与されたことがある人
6) 大きな手術を受けたことがある人
7) 臓器移植を受けたことがある人
8) 薬物濫用者，入れ墨（タトゥー）をしている人
9) ボディピアスを施している人
10) その他（過去に健康診断などで肝機能検査の異常を指摘されているにも関わらず，その後肝炎の検査を実施していない人など）

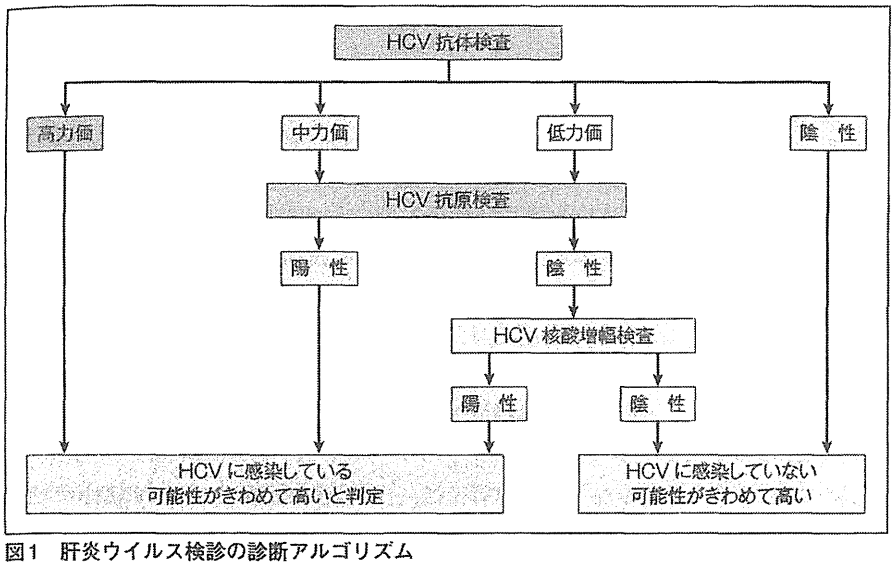

図1 肝炎ウイルス検診の診断アルゴリズム

3. C型慢性肝炎の抗ウイルス療法の治療効果予測

インターフェロンなどによる抗ウイルス療法による治療効果は，血中のHCV量が少ない方がより効果が高いとされる．このため抗ウイルス療法を考慮する際にはHCVコア抗原検査または核酸増幅検査によるHCV定量検査を実施し，治療効果を予測し治療方針を決定する．

4. C型慢性肝炎抗ウイルス療法の治療効果判定

インターフェロンなどによる抗ウイルス療法中には血中HCV量は動的に変化することが知られている[1]．この治療中のHCV動態をモニターすることで治療効果が予測でき，それに基づいて治療法の最適化が行われている．HCV動態のモニターには，高感度で定量性の高いHCV検査法が必要でありHCVコア抗原検査法やリアルタイムPCRによるHCV核酸増幅検査が用いられる．治療早期の血中HCV量の減衰が早く，血中HCV-RNAが早く陰性化する症例ほど最終的治療効果が高い．

また，抗ウイルス療法によりHCVが排除されC型肝炎が治癒したか否かの判定には，リアルタイムPCR法によるHCV核酸増幅検査を用いる．すなわち，抗ウイルス療法終了後6ヵ月時点でのHCV-RNAの陰性で判定される．ちなみに，抗ウイルス療法による治癒後ではHCV抗体は「高力価」陽性のことが多く，年単

位の経過を経て抗体価は徐々に低下する.

3 悩ましいときの次の一手

1. HCVの急性感染

HCV感染直後では，HCVの感染状態でもHCV抗体が陰性のことがある．一般にHCV感染からHCV抗体陽性となる期間(HCV抗体のウィンドウ期)は約3ヵ月である．したがって，C型急性肝炎のHCV抗体陽性率は発症時で50～70％，3ヵ月後は約90％である．わが国では，新規のHCV感染の発生が少なくはなってきたが，HCV抗体陰性でもHCVの急性感染を疑った場合は，核酸増幅検査でHCV-RNAを測定し診断する必要がある．なお，HCV感染からHCV-RNA陽性となる期間は約23日である.

また，血液透析患者や免疫不全患者では，HCV感染状態でもHCV抗体が陰性のことがあるので注意を要する.

2. HCV感染状態と診断されたときのさらなるウイルス学的検査

HCV抗体検査やHCVコア抗原および核酸増幅検査でHCV感染状態と判定された場合には，治療適応や治療方針の決定のために，専門医によりさらなるウイルス学的検査が行われる.

1) HCVゲノタイプ検査

HCVは6つのゲノタイプと，さらにそれぞれサブゲノタイプに分かれる．HCVゲノタイプの違いにより抗ウイルス療法の治療成績が異なるため，治療方針を決定するためにゲノタイプの同定検査がきわめて重要である．わが国には，ゲノタイプ1b，2a，2bが存在し，頻度は1bが70％，2aが20％，2bが10％を占める．インターフェロンの感受性は，ゲノタイプ2a＞2b＞1bの順に高い.

2) セロタイプ

NS3およびNS4領域の抗原であるC14-1およびC14-2抗原を用いたELISA法により測定し保険適用がある．一般的にセログループ1はゲノタイプ1に，セログループ2はゲノタイプ2に相当する．したがって，インターフェロンの感受性はセログループ2の方がセログループ1に比し高い.

3) NS5A変異

HCVゲノタイプ1bにおいて，HCV遺伝子の非構造領域であるNS5Aの後半部に存在するアミノ酸コドン2,209～2,248の40アミノ酸の変異数がインターフェロン療法の治療効果と密接に関連しており，インターフェロン感受性決定領域

(interferon sensitivity determining region：ISDR)と名づけられている[2,3]．ゲノタイプ1bのプロトタイプであるHCV-Jと比べて，ISDRにアミノ酸変異を多く認めるほどインターフェロンの治療効果が高い．ISDRの変異数は直接塩基配列決定法によって測定される．

4) HCVコア変異

HCVゲノタイプ1bにおいて，HCV遺伝子の構造領域であるコア遺伝子のアミノ酸コドン70番と91番のアミノ酸変異がインターフェロン療法の治療効果と密接に関連していることが知られている[4]．コア70番や91番にアミノ酸変異を認める変異型のHCVは，変異を認めない野生型のHCVに比し，インターフェロン抵抗性である．

5) 宿主のIL28B遺伝子近傍の1遺伝子多型(SNP)

宿主の19番染色体上に存在しインターフェロンλをコードしているIL28B遺伝子の近傍に存在するSNPが，インターフェロン・リバビリン併用療法の治療効果やHCV急性感染時における自然排除に，きわめて強く関連していることが最近発見された[5~7]．したがって，HCVキャリアと診断され抗ウイルス療法を考慮する際には，患者の同意を得た上で測定されることがある．

●参考文献●

1) Asahina Y, Izumi N, Uchihara M, et al : A potent antiviral effect on hepatitis C viral dynamics in serum and peripheral blood mononuclear cells during combination therapy with high-dose daily interferon alfa plus ribavirin and intravenous twice-daily treatment with interferon beta. Hepatology 2001 ; 34 : 377-384
2) Enomoto N, Sakuma I, Asahina Y, et al : Comparison of full-length sequences of interferon-sensitive and resistant hepatitis C virus 1b. Sensitivity to interferon is conferred by amino acid substitutions in the NS5A region. J Clin Invest 1995 ; 96 : 224-230
3) Enomoto N, Sakuma I, Asahina Y, et al : Mutations in the nonstructural protein 5A gene and response to interferon in patients with chronic hepatitis C virus 1b infection. N Engl J Med 1996 ; 334 : 77-81
4) Akuta N, Suzuki F, Sezaki H, et al : Association of amino acid substitution pattern in core protein of hepatitis C virus genotype 1b high viral load and non-virological response to interferon-ribavirin combination therapy. Intervirology 2005 ; 48 : 372-380
5) Tanaka Y, Nishida N, Sugiyama M, et al : Genome-wide association of IL28B with response to pegylated interferon-alpha and ribavirin therapy for chronic hepatitis C. Nat Genet 2009 ; 10 : 1105-1109
6) Ge D, Fellay J, Thompson AJ, et al : Genetic variation in IL28B predicts hepatitis C treatment-induced viral clearance. Nature 2009 ; 461 : 399-401
7) Thomas DL, Thio CL, Martin MP, et al : Genetic variation in IL28B and spontaneous clearance of hepatitis C virus. Nature 2009 ; 461 : 798-801

(朝比奈靖浩)

肝臓病診療ゴールデンハンドブック 改訂第2版

編集 泉 並木